MODERN ASTRONOMY:
FROM THE EARLY UNIVERSE TO EXOPLANETS AND BLACK HOLES

# Multi-wavelength observations of the impulsive C2.8 class flare producing photospheric impact at the penumbra region of the leading sunspot in NOAA 13256

G. Koynash[1], I. Sharykin[1], I. Zimovets[1], E. Ivanov[2], V. Kiselev[2], and B. Nizamov[3]

[1] Space Research Institute of Russian Academy of Sciences, Moscow, 117997 Russia
[2] Institute of Solar-Terrestrial Physics of Siberian Branch of Russian Academy of Sciences, Lermontov st., 126a, Irkutsk, 664033 Russia
[3] Sternberg Astronomical Institute, Universitetsky pr., 13, Moscow, 119234 Russia

**Abstract.** We present the results of a study of the non-eruptive C2.8 class flare in the active region (AR) NOAA 13256, which occurred on March 19,2023 from 02:12 to 02:19 UTC. This event was chosen on the basis of the test launches of the Irkutsk Solar Radio Spectropolarimeter (SOLARSPEL), Badary (ISTP RAS). Despite the low X-ray class and short duration, according to SOLARSPEL data, this impulsive flare had a complex multi-peak fine time structure, recorded at different frequencies in the microwave range. The presence of a photospheric disturbance in the vicinity of the sunspot penumbra, recorded using HMI/SDO, was of great interest for physics and motivated this study. There are few detailed multi-wavelength studies in the literature of low-power flares accompanied by a response at the photosphere level. Notably, this event was observed simultaneously by four X-ray instruments: SoLO/STIX, ASO-S/HXI, FERMI/GBM, and Konus-Wind. As a result, the unique observation conditions of this flare, from the point of view of the available instruments and various recorded physical high-energy processes, motivated us to carry out detailed research. We found that the photospheric perturbations are mostly associated with the stronger magnetic field in the penumbra rather than with the distribution of the HXR sources. The observed flare ribbons were located in the penumbral PIL region, which revealed the complexity of the larger events in terms of the spatial and temporal structure of the energy release. We also briefly discuss the observed quasi-periodic pulsations.

**Keywords:** Sun: solar flare, radio emission, X-ray emission, photospheric perturbations, magnetic fields

**DOI:** 10.26119/VAK2024.108

## 1 Introduction

The selected solar flare (briefly described in the abstract) is investigated due to the following peculiarities that motivated us for this research: relatively low GOES class, multi-peak impulsive energy release in the MW data, presence of photospheric impacts, and relatively simple AR morphology. Moreover, we have an abundance of observational data, making this flare unique for collecting detailed physical information. Today, there are not as many complex case studies of solar flares below the C3.0 class that are accompanied by photospheric perturbations (e.g., Song et al. 2020) in active regions with simple Hale and McIntosh classes. Furthermore, flares with white-light emission and photospheric perturbations are quite rare in the case of C-class flares (see, the statistical work of Song & Tian 2018). The main aim is to study the morphological properties of this particular solar flare: the configuration of the emission sources in the multi-wavelength data relative to each other in the AR and to the positions of the photospheric impacts and magnetic field structure.

## 2 Observations and Instruments

A selected C2.8 solar flare occurred near the eastern limb (S23E58) in AR NOAA 13256, on March 19, 2023. It began at 02:12 UT, reached its maximum at 02:14:54 UT, and ended at 02:19 UT. The parent AR, where the flare was located, had a Hale $\beta$ class and a "simple" McIntosh class of Eho, with the magnetic field flux concentrated in a large single leading sunspot, where flare emission sources were also detected. We also registered photospheric disturbances seen in HMI 45 second data: line-of-sight (LOS) magnetograms and Dopplergrams.

This flare was simultaneously observed with the Solar Radio Spectropolarimeter (SOLARSPEL), the Nobeyama Radio Polarimeters (NoRP, Nakajima et al. 1985); Siberian Radio Heliograph (SRH, Altyntsev et al. 1985), the Atmospheric Imaging Assembly (AIA, Lemen et al. 2012), the Helioseismic and Magnetic Imager (HMI, magnetic field and mapping of photospheric impacts, Scherrer et al. 2012) onboard the Solar Dynamics Observatory (SDO); the X-Ray Sensor (XRS) onboard the Geostationary Operational Environmental Satellite (GOES), the Gamma Ray Burst Monitor (GBM, Meegan et al. 2009) onboard the FERMI, the Konus/Wind (Aptekar et al. 2009), the Spectrometer Telescope for Imaging X-rays (STIX, Krucker et al. 2020) on the Solar Orbiter and the Hard X-Ray Imager (HXI, Zhang et al. 2019) on the Advanced Space-based Solar Observatory.

SOLARSPEL is a new radio broadband spectropolarimeter located at the Badary Radioastrophysical Observatory, and its data obtained from test runs allowed us to identify the studied flare due to its impulsive multi-peak MW time series (from event

catalog of the SOLARSPEL test runs). SOLARSPEL and NoRP measure microwave (MW) emission from the entire Sun in multiple frequency channels. The MW flux is measured for a frequency grid of 48 channels in the range from 3 GHz to 24 GHz (for the studied flare, only the 3–12 GHz range is available) with circular polarization for SOLARSPEL with a time cadence of 1 s, and intensity and circular polarization at six frequencies (we detected a polarization signal only at 9.4 GHz) for NoRP with a time cadence of 0.1 s. Periodic background variations in SOLARSPEL data are due to not well-compensated instrumental effects.

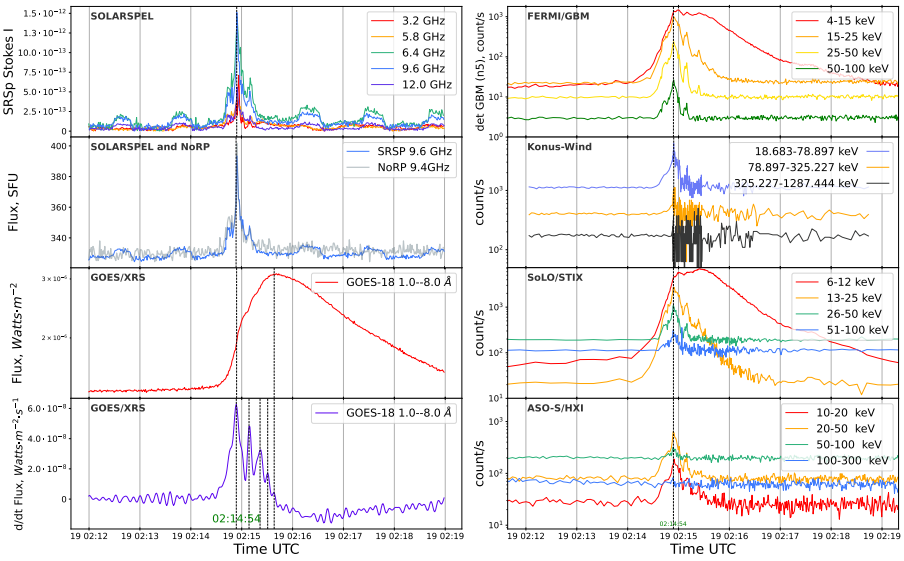


**Fig. 1.** Overview of the time profiles (TP) of the C2.8 GOES-class solar flare on March 19, 2023 from 02:12 to 02:19 UT. Left side: the SOLARSPEL, NoRP, GOES/XRS TSs and the time derivative of GOES/XRS. Right side: Fermi/GBM, Konus-Wind, SoLO/STIX and ASO-S/HXI.

Figure 1 shows the light curves produced by the mentioned instruments. In top left corner, we present the uncalibrated SOLARSPEL MW data at five frequencies (Stokes I). Below them are the NoRP's MW data for 9.4 GHz and the SOLARSPEL MW data at 9.6 GHz, calibrated with the NoRP's 9.4 GHz data.

## 3 Data Analysis and Results

We analysed SOLARSPEL and NoRP MW data, finding pronounced polarization in the radio burst. SOLARSPEL showed good sensitivity and temporal resolution with

consistent signals across a wide frequency range. Although we lacked sufficient data to fully calibrate the SOLARSPEL.

The MW and X-ray data reveal that the flare's impulsive phase consisted of a few peaks. In general, X-ray observations are consistent with the Neupert effect. Based on those data, we detected quasi-periodic pulsations (QPP) with a repeat period $P_{\rm R} \approx 12.3 \pm 2.5$ s. QPP is a common feature of flaring energy releases in the solar atmosphere, observed in all bands, from radio and MW to hard X-rays and gamma-rays (Nakariakov & Melnikov 2009). The physical mechanisms responsible for QPP can be explained by various models (e.g., Zimovets et al. 2021). For this episode, we plan to investigate it more carefully and in detail later.

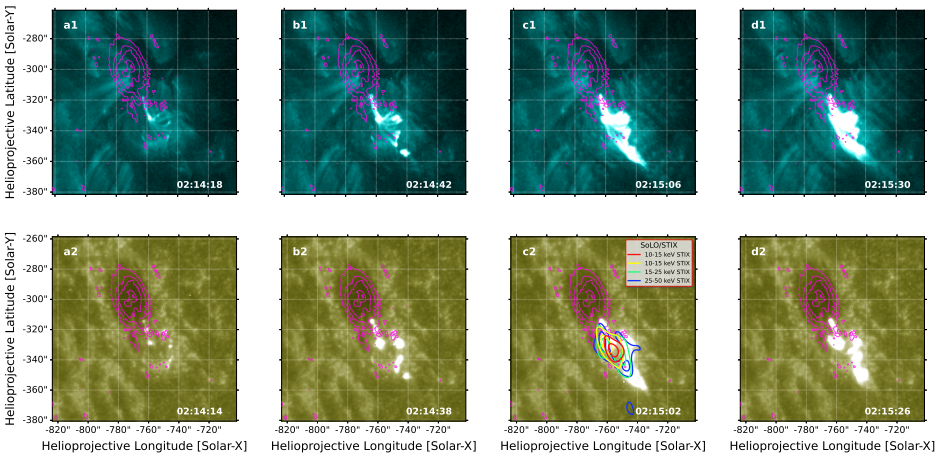


**Fig. 2.** The sequence of image snapshots with a field of view (FOV) of 130" × 130" of the C2.8 flare observed by SDO/AIA (EUV 131 Å – top row; UV 1600 Å – bottom row) includes SDO/HMI contours of magnetic field [1.0, 1.5, 2.0, 2.5, 3.0] kG, and contours for X-ray energy bands: 4–10 keV (red), 10–15 keV (yellow), 15–25 keV (green), 25–50 keV (blue).

However, these peaks could be connected with the multiple magnetic loops forming a magnetic arcade. To analyse the spatial structure of the flare energy release with the best available spatial resolution, we used AIA images (Fig. 2) at 131 Å (top–Fig. 2) with a time cadence of 12 s, and a low-temperature chromospheric UV band around 1600 Å(bottom–Fig. 2), with a time cadence of 24 s. In 1600 Å, we observe many localized quasi-static brightnings forming large-scale flare ribbons, with the northern one located in the sunspot penumbra. It is noteworthy that the small event shows "complexity" characteristic of large flares and cannot be considered as an "elementary" episode of flare energy release.

The STIX X-ray contour images are shown in Fig. 2(c2). We observe a typical situation with two HXR sources corresponding to the flare ribbons. A more detailed vizualization of high-energy flare processes is presented in Fig. 3. MW contour images from SRH at a few frequencies, X-ray STIX and HXI contour maps cover the AIA 1600 Å map at the flare MW peak in the corresponding figure panels (a–c). The spatial resolution of X-ray images is sufficient to resolve paired HXR sources. In the case of SRH, we observe a single flare source covering the flare UV ribbons or located between the ribbons at the highest frequencies. Possibly, we observe MW coronal sources.

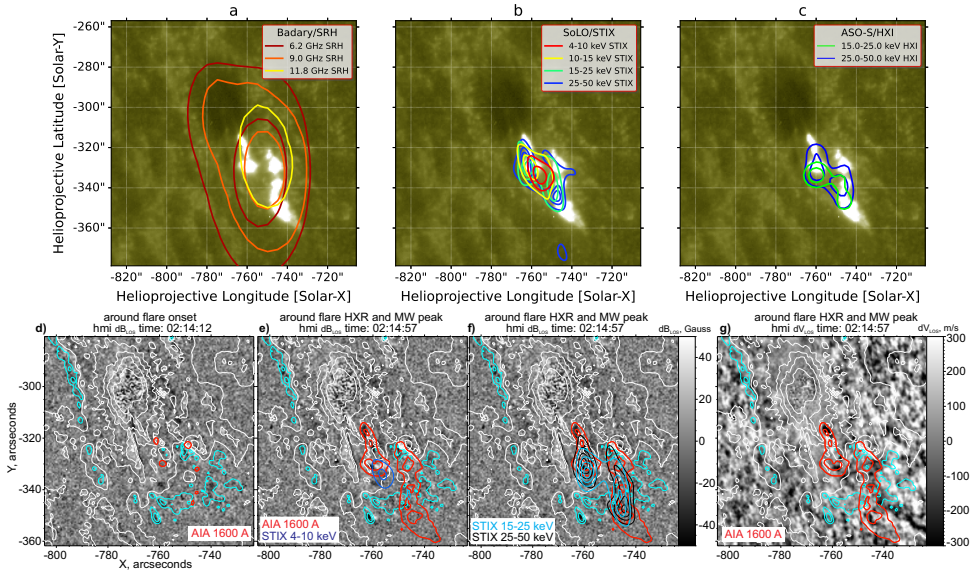


**Fig. 3.** Top panels show the AIA 1600 Å image with countours of SRH (a), STIX(b), HXI(c) sources. The bottom panels present photospheric perturbation observed in the HMI LOS magnetograms (d–f) and Dopplergram (g). Panel d corresponds to the flare onset, while panels (e–g) show the flare MW peak time. Red contours show the AIA 1600 Å emission sources. STIX contours are also shown in panels (e–f). Contours highlight magnetic field strengths of 1.0, 1.5, 2.0, 2.5, and 3.0 kG, with the PIL location marked by the thick white line. Different polarities are shown by white and cyan.

Weak photospheric perturbations were best observed in HMI 45-second LOS magnetograms and Dopplergrams (Fig. 3). The strongest impacts were detected in the northern ribbon (highlighted by the thick red contour in panel (e), associated with the stronger penumbral magnetic fields compared to the larger ribbon on the other side of the PIL outside the sunspot. It's worth noting that some photospheric perturbations are outside the centroids of the HXR sources (Fig. 3(f)). It seems that

the photospheric perturbation are related to the presence of the strong magnetic field. It is possible that we observe MHD motions of the magnetized plasma due to the magnetic reconnection process. However, it's also possible that some dense narrow beams of energetic particles are not seen in HXR due to the limited dynamic ranges of STIX and HXI. Additional research is needed to understand physics of the changing photospheric magnetic field and Doppler velocity in the flare ribbons.

## 4 Conclusions

The following conclusions for the studied flare were drawn:

1. The studied C2.8 flare reveals a complexity typical of large events despite the relatively simple morphology of the parent AR. There are two ribbons on either side of the penumbral polarity inversion line (PIL), corresponding hard X-ray sources, and a fine temporal and spatial structure of the energy release.
2. The nature of the observed MW and HXR QPPs is uncertain. The multi-peak time series may be explained by subsequent energy release in separate thin magnetic loops rooted at the flare ribbons, forming the observed fine spatial structure.
3. Photospheric perturbations are registered in the flare ribbon of the sunspot penumbra. There is no exact coincidence with the HXR emission sources. Are the flare photospheric impacts primarily connected with the magnitude and structure of the magnetic field?

**Acknowledgements.** We thank the numerous team members of the SRH and SOLARSPEL (Badary, ISTP RAS)[4], NoRP, SDO, GOES, STIX, HXI, GBM, and Konus-Wind for providing the data and corresponding analysis software.

## References

Altyntsev A.T., Lesovoi S., Globa M., et al., 2020, Solar-Terrestrial Physics, 6, 2, p. 30
Aptekar R.L., Cline T.L., Frederiks D.D., et al., 2009, Astrophysical Journal Letters, 698, 2, p. L82
Krucker Säm, Hurford G.J., Grimm O., et al., 2020, Astronomy & Astrophysics, 642, id. A15
Lemen J.R., Title A.M., Akin D.J., et al. 2012, Solar Physics, 275, 1-2, p. 17
Meegan C., Lichti G., Bhat P.N., et al., 2009, Astrophysical Journal, 702, 1, p. 791
Nakajima H., Sekiguchi H., Sawa M., et al., 1985, Publications of Astronomical Society of Japan, 37, p. 163
Nakariakov V.M. and Melnikov V.F., Space Science Reviews, 2009, 149, 1-4, p. 119
Scherrer P.H., Schou J., Bush R.I., et al., 2012, Solar Physics, 275, 1-2, p. 207.
Song Y., Tian H., Zhu X., et al., 2020, Astrophysical Journal Letters, 893, 1, id. L13
Song Y. and Tian H., 2018, Astrophysical Journal, 867, 2, id. 159
Zhang Z., Chen D.-Y., Wu J., et al., 2019, Research in Astronomy & Astrophysics, 19, 11, id. 160
Zimovets I.V., McLaughlin J.A., Srivastava A.K., et al., 2021, Space Science Reviews, 217, p. 66

[4] https://badary.iszf.irk.ru